molecules

MDPI

Article

Impact of Pd Loading on CO_2 Reduction Performance over Pd/TiO_2 with H_2 and H_2O

Akira Nishimura [1,*], Tadaaki Inoue [1], Yoshito Sakakibara [1], Masafumi Hirota [1], Akira Koshio [2] and Eric Hu [3]

1 Division of Mechanical Engineering, Graduate School of Engineering, Mie University, Tsu, Mie 514-8507, Japan; 418M109@m.mie-u.ac.jp (T.I.); 419M117@m.mie-u.ac.jp (Y.S.); hirota@mach.mie-u.ac.jp (M.H.)
2 Division of Chemistry for Materials, Graduate School of Engineering, Mie University, Tsu, Mie 514-8507, Japan; koshio@chem.mie-u.ac.jp
3 School of Mechanical Engineering, the University of Adelaide, SA 5005, Australia; eric.hu@adelaide.edu.au
* Correspondence: nisimura@mach.mie-u.ac.jp; Tel.: +81-59-231-9747; Fax: +81-59-231-9747

Academic Editor: Marcelo I. Guzman
Received: 21 February 2020; Accepted: 22 March 2020; Published: 24 March 2020

check for updates

Abstract: This study investigated the impact of molar ratio of CO_2 to reductants H_2O and H_2, as well as Pd loading weight on CO_2 reduction performance with Pd/TiO_2 as the photocatalyst. The Pd/TiO_2 film photocatalyst is prepared by the sol-gel and dip-coating process to prepare TiO_2 film and the pulse arc plasma method is used to dope Pd on TiO_2 film. The prepared Pd/TiO_2 film was characterized by SEM, EPMA, STEM, EDS, and EELS. This study also investigated the performance of CO_2 reduction under the illumination condition of Xe lamp with or without ultraviolet (UV) light. As a result, it is revealed that when the molar ratio of $CO_2/H_2/H_2O$ is set at 1:0.5:0.5, the best CO_2 reduction performance has been obtained under the illumination condition of Xe lamp with and without UV light. In addition, it is found that the optimum Pd loading weight is 3.90 wt%. The maximum molar quantities of CO and CH_4 produced per unit weight of photocatalyst are 30.3 μmol/g and 22.1 μmol/g, respectively, for the molar ratio of $CO_2/H_2/H_2O$ = 1:0.5:0.5 under the condition of Xe lamp illumination with UV light. With UV light, C_2H_4 and C_2H_6, as well as CO and CH_4 are also produced by the Pd/TiO_2 film photocatalyst prepared in this study.

Keywords: Pd/TiO_2 photocatalyst; CO_2 reduction; Pd loading weight; combination of reductants

1. Introduction

The Paris Agreement adopted in 2015 set the goal that the increase in average temperature in the world from the industrial revolution by 2030 should be kept less than 2 K. However, the global mean concentration of CO_2 in the atmosphere has increased up to 410 ppmV in December 2019, which increased by 25 ppmV since 2009 [1]. Therefore, it is requested to develop a new CO_2 reduction/utilization technology in order to reduce the amount of CO_2 in the atmosphere.

Reducing or converting CO_2 into fuel by photocatalyst became a hot R&D area. TiO_2 is commonly used as a photocatalyst for CO_2 reduction since it is convenient, inexpensive, and has strong durability for chemicals and corrosion [2]. TiO_2 is a popular photocatalyst that can reduce CO_2 into CO, CH_4, CH_3OH, and H_2 etc. with ultraviolet (UV) light [3–5].

Since pure TiO_2 can only be activated under UV light illumination, it is not very effective under sunlight illumination as UV light accounts for only approximately 4% in the solar spectrum. In addition, the rate of electron/hole pair recombination is faster than the rate of chemical interaction between the absorbents during redox reactions when using pure TiO_2 [6].

Many attempts have been reported to improve the performance of the TiO_2 [3]. Doping precious metals such as Pt [7], Ag [8], Au [9], Cu [10,11], using composite materials formed by GaP and TiO_2 [12], combining CdS/TiO_2 in order to utilize two photocatalysts that have different band gaps [13], adding carbon-based AgBr nanocomposites into TiO_2 [14], sensitizing $CuInS_2$ and TiO_2 hybrid nanofibers [15], and preparing a procedure of TiO_2 using two alcohols (ethanol and isopropyl alcohol) and supercritical CO_2 [16] are some of the attempts to promote the performance of TiO_2. Though the CO_2 reduction performance was improved to a certain degree in these attempts, the concentrations of the products were still low, which were ranging from 1 to 150 µmol/g-cat [7–16].

Among various metals that have been used for doping, Pd is considered as a favorite candidate [17–19], since Pd can extend the absorption band to 400–800 nm [20,21], which covers the whole visible light range. Pd/TiO_2 performs a higher reduction performance compared to pure TiO_2, especially, to produce hydrocarbon [20–22]. In addition, it is known that the CO_2 reduction performance of Pd/TiO_2 is superior to that of TiO_2 from the viewpoint of producing CH_4 and H_2 [7,19]. This is due to the work function of Pd, which reflects the electron donating or accepting ability. In addition, it is thought that Pd loaded on TiO_2 functions to increase the efficiency of photogenerated electrons for the formation of reductive products.

According to the literature survey, H_2O or H_2 were normally used as the reductants for CO_2 reduction over Pd/TiO_2 [17–23]. In studies of CO_2 reduction with H_2O [17–22], the mixture ratio of CO_2 and H_2O was fixed. According to the report on CO_2 reduction with H_2 [23], the molar ratio of CO_2:H_2 was fixed at 1:4, but the impact of the ratio on CO_2 reduction performance of Pd/TiO_2 was not investigated. Though it is thought that the mixture ratio of CO_2 and reductants influences the CO_2 reduction performance of Pd/TiO_2, there was no other study investigating it nor the effect of using both H_2O and H_2 as reductants on CO_2 reduction over Pd/TiO_2 except the study conducted by the authors [24]. In addition, the metal loading weight with TiO_2 is important to improve the CO_2 reduction performance [25,26]. However, there was no study so far to qualify the improvement.

To promote the CO_2 reduction performance, the optimum reductant providing the proton (H^+) should be clarified. According to the previous studies [27–30], the reaction mechanism to reduce CO_2 with H_2O can be summarized as shown below:

<Photocatalytic reaction>

$$TiO_2 + h\nu \rightarrow h^+ + e^- \tag{1}$$

<Oxidization>

$$2H_2O + 4h^+ \rightarrow 4H^+ + O_2 \tag{2}$$

<Reduction>

$$CO_2 + 2H^+ + 2e^- \rightarrow CO + H_2O \tag{3}$$

$$CO_2 + 8H^+ + 8e^- \rightarrow CH_4 + 2H_2O \tag{4}$$

$$2CO_2 + 12H^+ + 12e^- \rightarrow C_2H_4 + 4H_2O \tag{5}$$

$$2CO_2 + 14H^+ + 14e^- \rightarrow C_2H_6 + 4H_2O \tag{6}$$

The reaction mechanism to reduce CO_2 with H_2 can be summarized as shown below [30,31].

<Photocatalytic reaction>

$$TiO_2 + h\nu \rightarrow h^+ + e^- \tag{7}$$

<Oxidization>

$$H_2 \rightarrow 2H^+ + 2e^- \tag{8}$$

<Reduction>

$$CO_2 + e^- \rightarrow CO_2^- \tag{9}$$

$$CO_2^- + H^+ + e^- \rightarrow HCOO^- \tag{10}$$

$$HCOO^- + H^+ \rightarrow CO + H_2O \tag{11}$$

$$CO_2 + 8e^- + 8H^+ \rightarrow CH_4 + 2H_2O \tag{12}$$

$$2CO_2 + 12e^- + 12H^+ \rightarrow C_2H_4 + 4H_2O \quad (13)$$

$$2CO_2 + 14e^- + 14H^+ \rightarrow C_2H_6 + 4H_2O \quad (14)$$

Though a few studies using pure TiO_2 under $CO_2/H_2/H_2O$ condition were reported [32–34], the effect of ratio of CO_2, H_2, and H_2O, as well as the effect of Pd loading on CO_2 reduction characteristics was not investigated previously.

The purpose of this study is to clarify the effect of molar ratio of CO_2 to reductants of H_2 and H_2O on CO_2 reduction characteristics with Pd/TiO_2. Additionally, the present study also aims to clarify the optimum combination of reductants, as well as Pd loading weight with TiO_2.

The present study employed TiO_2 films coated on netlike glass fibers (SILIGLASS U, Nihonmuki Co., Tokyo, Japan) by the sol-gel and dip-coating process. The glass fiber whose diameter is about 10 μm is weaved as a net, resulting in the diameter of collected fiber of approximately 1 mm. As to the specification of each fiber, the porous diameter is approximately 1 nm and the specific surface area is approximately 400 m^2/g. The composition of netlike glass fiber is SiO_2 of 96 wt%. The aperture area is approximately 2 mm × 2 mm. Due to the porous structure of the netlike glass fiber, the TiO_2 film can be captured on netlike glass fiber easily in the step of preparation by sol-gel and dip-coating procedure. Additionally, it was believed that CO_2 would be more easily absorbed by the prepared photocatalyst since the porous fiber has a large surface area [35,36].

After the coating of TiO_2, nanosized Pd particles were loaded on TiO_2 by the pulse arc plasma method applying high voltage. The pulse number can be controlled by the quantity of Pd loaded. The Pd loading weight on TiO_2 was measured by Electron Probe Micro Analyzer (EPMA).

In this paper, the characterization of Pd/TiO_2 was conducted by Scanning Electron Microscope (SEM), EPMA, Scanning Transmission Electron Microscope (STEM), Energy Dispersive X-ray Spectrometer (EDS), and Electron Energy Loss Spectrum (EELS) analysis before the CO_2 reduction experiment. The performances of CO_2 reduction with H_2 and H_2O under the condition of illuminating Xe lamp including or excluding UV light were investigated in this paper. The combination of $CO_2/H_2/H_2O$ was changed for 1:0.5:0.5, 1:0.5:1, 1:1:0.5, 1:1:1, and 1:2:2 based on molar ratio to clarify the optimum combination of $CO_2/H_2/H_2O$ for CO_2 reduction with Pd/TiO_2. If the amount of H_2 is larger than that of H_2O, it is thought that the effect of H_2O on the photocatalytic reaction is higher. On the other hand, if the amount of H_2O is larger than that of H_2, it is thought that the effect of H_2O on the photocatalytic reaction is higher. This study investigated the effect of H_2 or H_2O on the CO_2 reduction performance of Pd/TiO_2 under the condition of $CO_2/H_2/H_2O$ for the first time, so the originality of this study could be justified. In addition, the effect of Pd loading weight with TiO_2 on CO_2 reduction performance was also investigated in this study.

2. Results and Discussion

2.1. Characterization Analysis of Pd/TiO_2 Film

Figure 1, Figure 2 show SEM images of TiO_2 film and Pd/TiO_2 film coated on netlike glass disc, respectively. The SEM images were taken at 1500 times magnification. In these figures, the red circles indicate TiO_2 according to EPMA results. Figures 3 and 4 show EPMA results of TiO_2 and Pd/TiO_2 film coated on netlike glass disc, respectively. The data with the weight percentage of Pd to Pd/TiO_2 film of 4.97 wt% are shown in Figure 4 as an example. In these figures, the different colors indicate the concentrations of each element in the observation area. For example, light colors such as white, pink, and red mean the quantity of element is small.

According to these figures, it is clear that TiO_2 film was coated on netlike glass fiber. In addition, it is observed that the crack is formed on the TiO_2 film. Since the thermal conductivity is different between Ti and SiO_2, which are 19.4 W/(m K) and 1.82 W/(m K), respectively at 600 K [37], the temperature distribution of TiO_2 solution adhered on the netlike glass disc was not uniform during the firing process, as a result, cracks were formed on the TiO_2 film by the thermal expansion and shrinkage around netlike glass fiber. As to the crystal structure of TiO_2, it is thought to be anatase since the firing temperature was set at 623 K in this study. A previous study [38] found the crystal structure of prepared TiO_2 was anatase if the firing temperature was from 673 K to 873 K, while it would be rutile if the firing temperature was 973 K. The uniform loading of nanosized Pd particles on TiO_2 was observed according to Figure 3.

The observation area of diameter of 300 μm is analyzed by EPMA to evaluate the quantity of loaded Pd within TiO_2 film. Twenty observation points obtained from several samples were used to determine the weight percentages of Pd and Ti in this study. As a result, the weight percentages of Pd to Pd/TiO_2 film prepared by changing pulse number in this study are 0.49 wt%, 3.90 wt%, and 4.97 wt%, while the weight percentage of Ti are 99.51 wt%, 96.10 wt%, and 95.03 wt%, respectively.

Figure 1. SEM result of TiO_2 film coated on netlike glass disc.

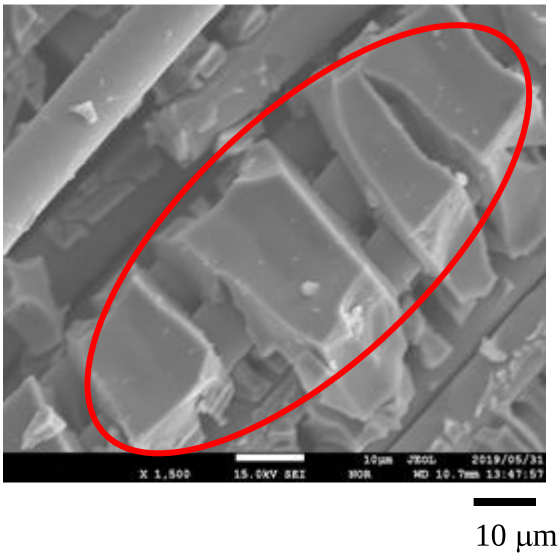

Figure 2. SEM result of Pd/TiO_2 film coated on netlike glass disc.

Figure 5 shows STEM and EDS results of Pd/TiO_2 film coated on netlike glass disc. 250,000 times magnification STEM image was used for the EDS analysis. It is observed that Pd is coated on TiO_2 film according to STEM image, which is confirmed from EDS image. It is also observed that the layout of Pd and Ti are separated. The thickness of the Pd coated is approximately 60 nm. Nanosized Pd particles are loaded on TiO_2 dispersedly.

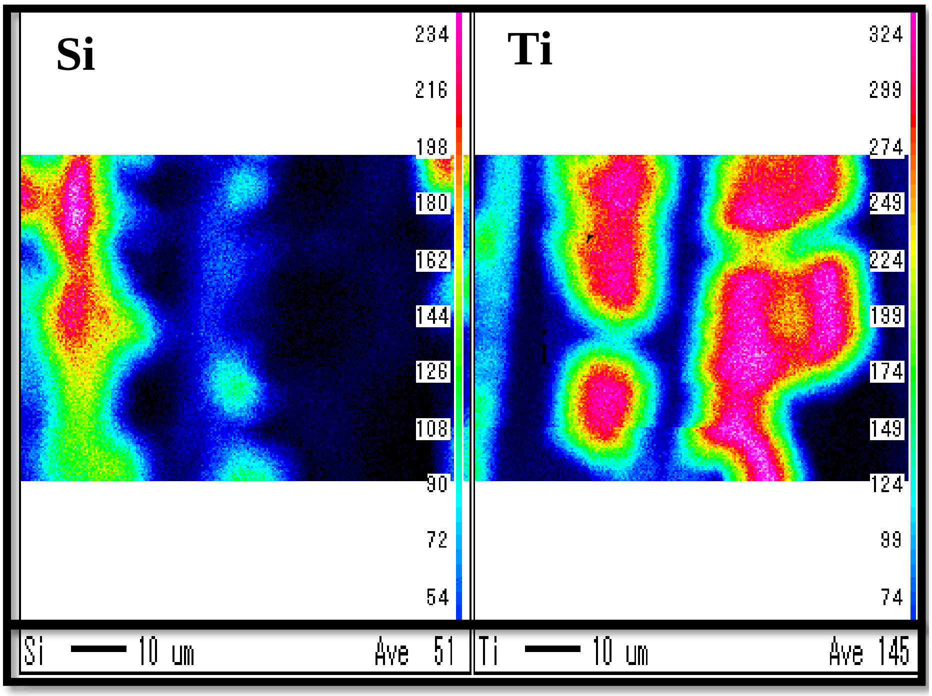

Figure 3. EPMA result of TiO_2 film coated on netlike glass disc.

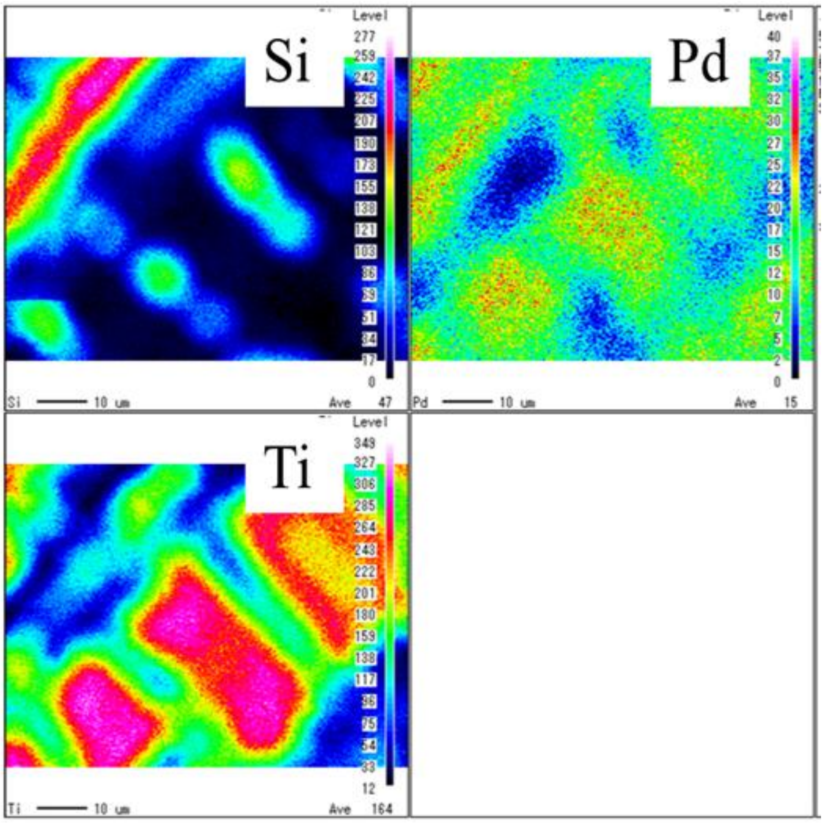

Figure 4. EPMA result of Pd/TiO_2 film coated on netlike glass disc.

Figure 6 shows EELS spectra of Pd in Pd/TiO_2 film which peaks at around 540 eV. Comparing the spectra peaks of Pd nanowire with that of Pd metal and PdO in [39], the EELS spectra of Pd metal matches that in Figure 6. Therefore, it is believed that the Pd in Pd/TiO_2 prepared in this study exists as

Pd metal. Since the photoreduction performance of Pd/TiO_2 was higher than that of PdO/TiO_2 [40,41], the desirable Pd/TiO_2 without oxidization was proved to be prepared in this study.

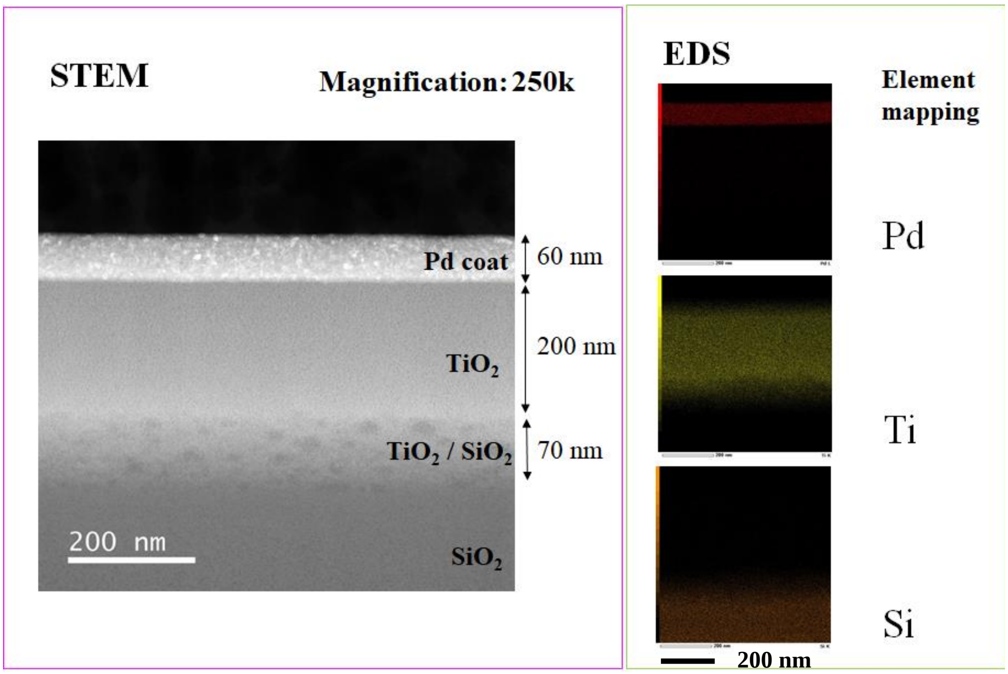

Figure 5. STEM and EDS analysis result of Pd/TiO_2 film coated on netlike glass disc.

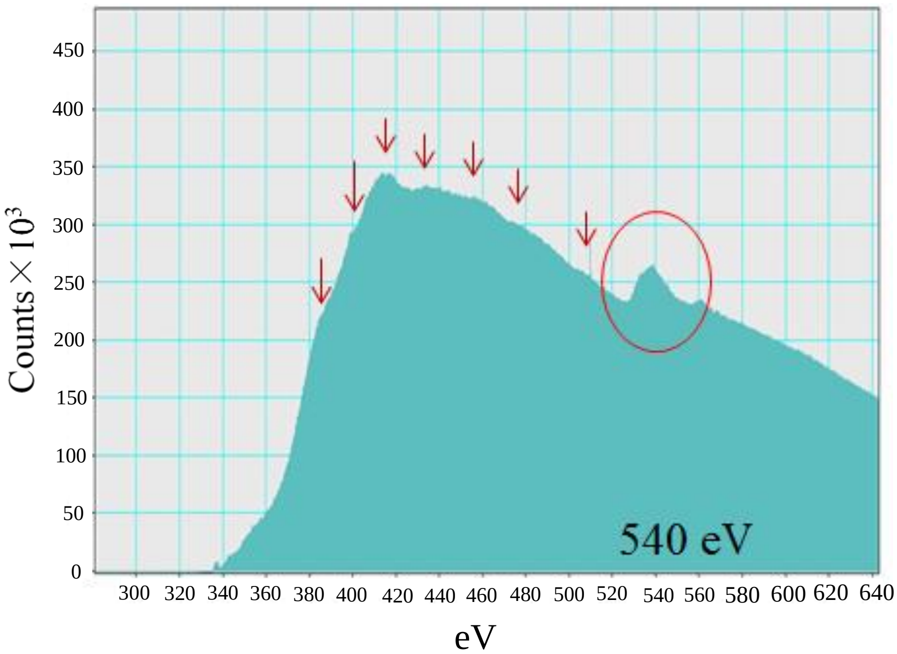

Figure 6. EELS spectra of Pd in Pd/TiO_2.

2.2. Impact of Molar Ratio of CO_2, H_2, and H_2O, as well as Pd Loading Weight on CO_2 Reduction Performance

Figures 7–10 show the change in concentration of formed CO, CH_4, C_2H_4, and C_2H_6 with Pd/TiO_2 film coated on netlike glass disc with the time under the condition of Xe lamp illumination with UV light, respectively. In these figures, the impact of molar ratio of CO_2, H_2, and H_2O, as well as Pd loading weight are also presented. Before this experiment, a blank test without Xe lamp illumination had been carried out as a reference, resulting that no fuel was detected as expected. Tables 1–4 list the maximum concentration of formed CO, CH_4, C_2H_4, and C_2H_6 under the condition shown in Figures 7–10, respectively.

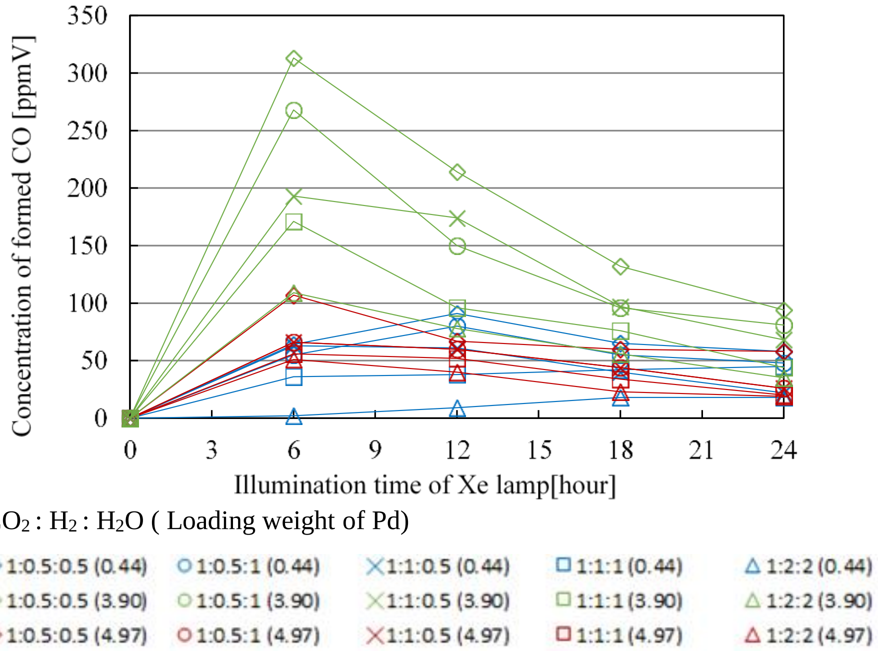

Figure 7. Change in concentration of formed CO with the illumination time among different molar ratios of $CO_2/H_2/H_2O$ and Pd loading weight with ultraviolet (UV) light illumination.

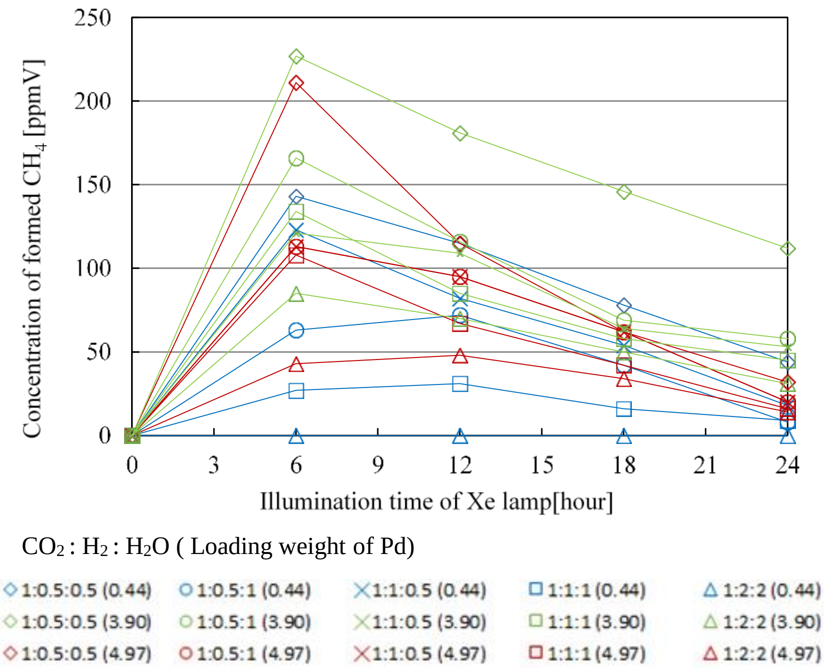

Figure 8. Change in concentration of formed CH_4 with the illumination time among different molar ratios of $CO_2/H_2/H_2O$ and Pd loading weight with UV light illumination.

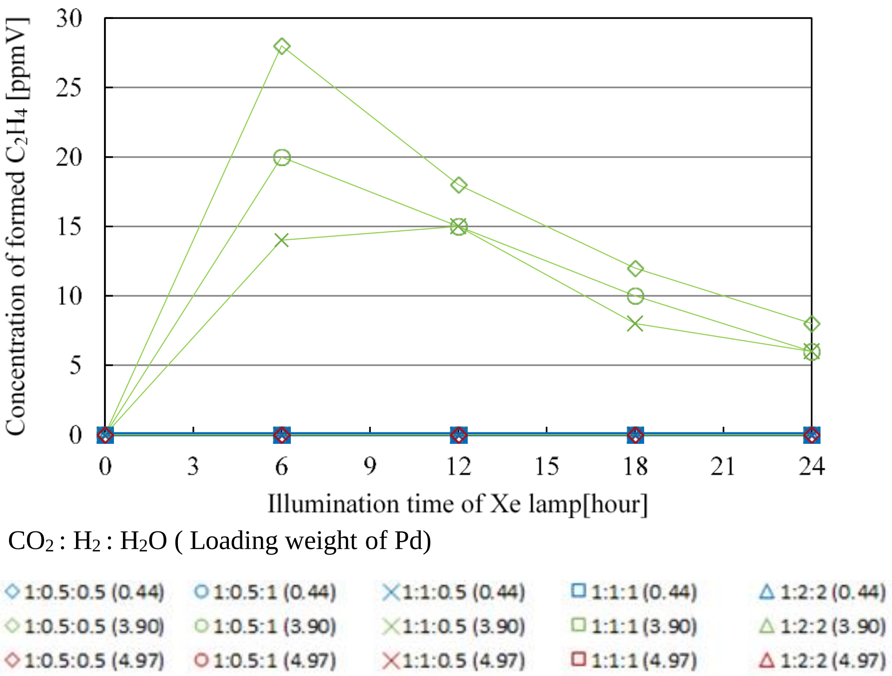

Figure 9. Change in concentration of formed C_2H_4 with the illumination time among different molar ratios of $CO_2/H_2/H_2O$ and Pd loading weight with UV light illumination.

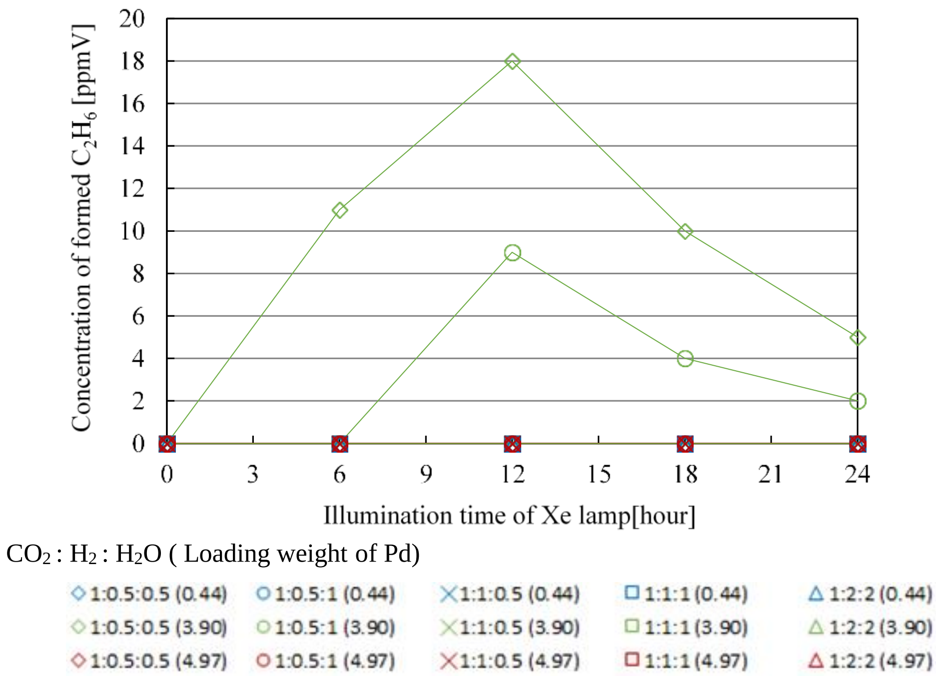

Figure 10. Change in concentration of formed C_2H_6 with the illumination time among different molar ratios of $CO_2/H_2/H_2O$ and Pd loading weight with UV light illumination.

Table 1. Comparison of maximum concentration of formed CO with illumination time among different molar ratios of $CO_2/H_2/H_2O$ and Pd loading weight with UV light illumination.

	1:0.5:0.5	1:0.5:1	1:1:0.5	1:1:1	1:2:2
0.44 wt%	91 ppmV	80 ppmV	63 ppmV	45 ppmV	18 ppmV
3.90 wt%	313 ppmV	268 ppmV	193 ppmV	171 ppmV	109 ppmV
4.97 wt%	107 ppmV	66 ppmV	66 ppmV	56 ppmV	51 ppmV

Table 2. Comparison of maximum concentration of formed CH_4 with illumination time among different molar ratios of $CO_2/H_2/H_2O$ and Pd loading weight with UV light illumination.

	1:0.5:0.5	1:0.5:1	1:1:0.5	1:1:1	1:2:2
0.44 wt%	143 ppmV	72 ppmV	123 ppmV	31 ppmV	0 ppmV
3.90 wt%	227 ppmV	166 ppmV	121 ppmV	134 ppmV	85 ppmV
4.97 wt%	211 ppmV	113 ppmV	113 ppmV	108 ppmV	48 ppmV

Table 3. Comparison of maximum concentration of formed C_2H_4 with illumination time among different molar ratios of $CO_2/H_2/H_2O$ and Pd loading weight with UV light illumination.

	1:0.5:0.5	1:0.5:1	1:1:0.5	1:1:1	1:2:2
0.44 wt%	0 ppmV	0 ppmV	0 ppmV	0 ppmV	0 ppmV
3.90 wt%	28 ppmV	20 ppmV	15 ppmV	0 ppmV	0 ppmV
4.97 wt%	0 ppmV	0 ppmV	0 ppmV	0 ppmV	0 ppmV

Table 4. Comparison of maximum concentration of formed C_2H_6 with illumination time among different molar ratios of $CO_2/H_2/H_2O$ and Pd loading weight with UV light illumination.

	1:0.5:0.5	1:0.5:1	1:1:0.5	1:1:1	1:2:2
0.44 wt%	0 ppmV	0 ppmV	0 ppmV	0 ppmV	0 ppmV
3.90 wt%	18 ppmV	9 ppmV	0 ppmV	0 ppmV	0 ppmV
4.97 wt%	0 ppmV	0 ppmV	0 ppmV	0 ppmV	0 ppmV

According to Figures 7–10 and Tables 1–4, the CO_2 reduction performance to produce CO, CH_4, C_2H_4, and C_2H_6 is the highest at the molar ratio of $CO_2/H_2/H_2O$ = 1:0.5:0.5. Since the reaction scheme of $CO_2/H_2/H_2O$ has not been fully understood, Equations (1)–(15) are used to explain the results. Equations (1)–(15) show that the theoretical molar ratio of CO_2 with H_2O or H_2 to produce CO is 1:1. On the other hand, the theoretical molar ratio of CO_2 with H_2O or H_2 to produce CH_4 is 1:4. In addition, CH_4, C_2H_4, and C_2H_6 are produced in the series after CO is produced. For example, producing CH_4 needs four times H^+ and electrons as many as producing CO needs. The other fuels such as C_2H_4 and C_2H_6 need more H^+ and electrons compared to producing CH_4. Since Pd has a high reduction performance [21,22,40], it is thought that the optimum molar ratio of CO_2/total reductants to produce CH_4, C_2H_4, and C_2H_6 is smaller than the theoretical molar ratio required. Moreover, since the molar ratio of H_2 is the same as that of H_2O under the molar ratio of $CO_2/H_2/H_2O$ = 1:0.5:0.5 condition, the effect of H_2 or H_2O is not higher than that of the other to obtain the optimum molar ratio of $CO_2/H_2/H_2O$ over Pd/TiO_2 photocatalyst. However, according to Tables 1–4, the CO_2 reduction performance for the condition that the molar ratio of H_2O is larger than that of H_2 is better, resulting in that the effect of H_2O is bigger than that of H_2 to promote the CO_2 reduction performance over Pd/TiO_2 totally in this study.

In addition, it is known from Figures 7–10 and Tables 1–4 that the maximum concentration of produced fuel is obtained when Pd loading weight is 3.90 wt% irrespective of fuel type. One might think that the CO_2 reduction performance is promoted with increasing Pd loading weight. However, it is believed that too much Pd loading causes covering the surface of TiO_2 film [42,43], resulting in that CO_2 and reductants cannot attain the surface of TiO_2 film sufficiently. Consequently, it is clear that there is an optimum Pd loading weight to promote CO_2 reduction performance with H_2 and H_2O.

Tables 5–8 list the maximum molar quantities of CO, CH_4, C_2H_4, and C_2H_6 per unit weight of photocatalyst under the condition of Xe lamp illumination with UV light, respectively. The quantities of Pd/TiO_2 coated on netlike glass disc for Pd loading weight of 0.44 wt%, 3.90 wt%, and 4.97 wt% are 0.05 g, 0.05 g, and 0.09 g, respectively. These quantities of Pd/TiO_2 coated on netlike glass disc were measured by an electric balance comparing the weights of several samples before and after preparing

Pd/TiO_2 film on netlike glass fiber. The photocatalytic activity evaluation using molar quantities of product per weight of photocatalyst was adopted as in the recent photocatalyst studies [44–47].

According to Tables 5–8, the maximum molar quantities of CO, CH_4, C_2H_4, and C_2H_6 per unit weight of photocatalyst are obtained for the molar ratio of $CO_2/H_2/H_2O$ = 1:0.5:0.5. In addition, it is known that the maximum molar quantity of fuel per unit weight of photocatalyst is obtained for Pd loading weight of 3.90 wt% irrespective of fuel type. It is thought that these results agree with the results shown in Figures 11–14.

Table 5. Comparison of the maximum molar quantity of CO per unit weight of photocatalyst with illumination time among different molar ratios of $CO_2/H_2/H_2O$ and Pd loading weight with UV light illumination (unit: µmol/g).

	1:0.5:0.5	**1:0.5:1**	**1:1:0.5**	**1:1:1**	**1:2:2**
0.44 wt%	9.27	8.18	9.06	4.63	1.81
3.90 wt%	30.4	26.0	18.9	16.6	10.6
4.97 wt%	5.97	3.66	3.52	3.10	2.84

Table 6. Comparison of the maximum molar quantity of CH_4 per unit weight of photocatalyst with illumination time among different molar ratios of $CO_2/H_2/H_2O$ and Pd loading weight with UV light illumination (unit: µmol/g).

	1:0.5:0.5	**1:0.5:1**	**1:1:0.5**	**1:1:1**	**1:2:2**
0.44 wt%	14.6	7.33	6.91	3.20	0
3.90 wt%	22.1	16.1	11.8	13.1	8.25
4.97 wt%	11.8	6.28	6.85	6.04	2.69

Table 7. Comparison of the maximum molar quantity of C_2H_4 per unit weight of photocatalyst with illumination time among different molar ratios of $CO_2/H_2/H_2O$ and Pd loading weight with UV light illumination (unit: µmol/g).

	1:0.5:0.5	**1:0.5:1**	**1:1:0.5**	**1:1:1**	**1:2:2**
0.44 wt%	0	0	0	0	0
3.90 wt%	2.69	1.91	1.46	0	0
4.97 wt%	0	0	0	0	0

Table 8. Comparison of the maximum molar quantity of C_2H_6 per unit weight of photocatalyst with illumination time among different molar ratios of $CO_2/H_2/H_2O$ and Pd loading weight with UV light illumination (unit: µmol/g).

	1:0.5:0.5	**1:0.5:1**	**1:1:0.5**	**1:1:1**	**1:2:2**
0.44 wt%	0	0	0	0	0
3.90 wt%	1.75	0.91	0	0	0
4.97 wt%	0	0	0	0	0

Figure 11 shows the change in concentration of formed CO with the Pd/TiO_2 film with the time under the condition of Xe lamp illumination without UV light. In this figure, the impact of molar ratio of CO_2, H_2, and H_2O, as well as Pd loading weight is also presented. Before this experiment, a blank test without Xe lamp illumination had been carried out as a reference, resulting in that no fuel was detected as expected. Table 9 lists the maximum concentration of formed CO under the condition shown in Figure 11.

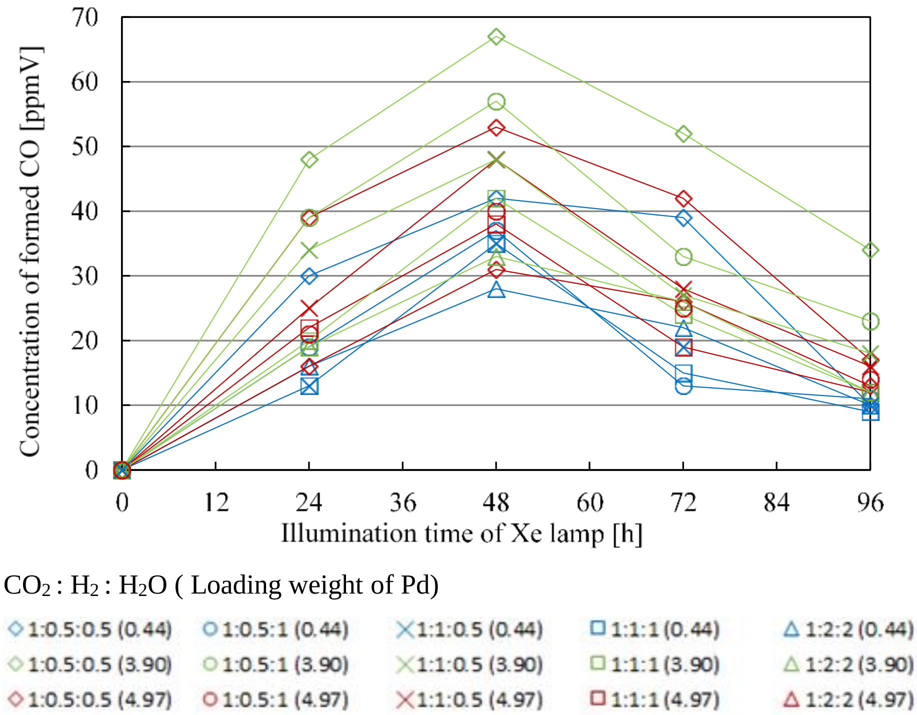

Figure 11. Change in concentration of formed CO with the illumination time among different molar ratios of $CO_2/H_2/H_2O$ and Pd loading weight without UV light illumination.

Table 9. Comparison of maximum concentration of formed CO with illumination time among different molar ratios of $CO_2/H_2/H_2O$ and Pd loading weight without UV light illumination.

	1:0.5:0.5	**1:0.5:1**	**1:1:0.5**	**1:1:1**	**1:2:2**
0.44 wt%	42 ppmV	37 ppmV	35 ppmV	35 ppmV	28 ppmV
3.90 wt%	67 ppmV	57 ppmV	48 ppmV	42 ppmV	33 ppmV
4.97 wt%	53 ppmV	40 ppmV	48 ppmV	38 ppmV	31 ppmV

According to Figure 11 and Table 9, the CO_2 reduction performance to produce CO is the highest at the molar ratio of $CO_2/H_2/H_2O$ = 1:0.5:0.5 and the maximum concentration of produced fuel is obtained for Pd loading weight of 3.90 wt%. These results are the same as that in the case of illuminating Xe lamp with UV light. The reason why these results are obtained is thought to be the same as explained above in the case of illuminating Xe lamp with UV light. It is found from Figure 11 that the concentration of formed CO is smaller than that under the condition of Xe lamp with UV light. There were no other fuels such as CH_4, C_2H_4, and C_2H_6 detected under the condition of Xe lamp illumination without UV light. It is thought that the responsiveness of visible light with Pd/TiO_2 prepared in this study was too low.

Table 10 shows the maximum molar quantity of CO per unit weight of photocatalyst under the condition of Xe lamp illumination without UV light. The maximum molar quantity of CO per unit weight of photocatalyst is obtained for the molar ratio of $CO_2/H_2/H_2O$ = 1:0.5:0.5 at Pd loading weight of 3.90 wt%. This result is the same as that in the case of illuminating Xe lamp with UV light.

Table 10. Comparison of maximum molar quantity of CO per unit weight of photocatalyst with illumination time among different molar ratios of $CO_2/H_2/H_2O$ and Pd loading weight without UV light illumination (unit: µmol/g).

	1:0.5:0.5	**1:0.5:1**	**1:1:0.5**	**1:1:1**	**1:2:2**
0.44 wt%	3.97	3.58	3.34	3.37	2.63
3.90 wt%	6.34	5.42	4.64	4.03	3.21
4.97 wt%	2.77	2.11	2.56	2.06	1.63

In this study, the maximum molar quantity of CH_4 per unit weight of photocatalyst is 22.1 μmol/g for the molar ratio of $CO_2/H_2/H_2O$ = 1:0.5:0.5 at Pd loading weight of 3.90 wt% under the condition of Xe lamp illumination with UV light. This maximum value is obtained after 6 h of illumination. According to the previous studies reported, the molar quantities of CH_4 per unit weight of photocatalyst in the case of CO_2/H_2O with Pd/TiO_2 were 25 μmol/g, 4.8 μmol/g, and 1.9 μmol/g [21,22,40]. These molar quantities of CH_4 per unit weight of photocatalyst were obtained after 8 [21], 6 [22], and 24 [40] h of illumination, respectively. Another study [23] reported that the molar quantity of CH_4 per unit weight of photocatalyst in the case of CO_2/H_2 with Pd/TiO_2 was 356 μmol/g which was obtained after 3 h of illumination.

In this study, the maximum molar quantity of CO per unit weight of photocatalyst is 30.3 μmol/g for the molar ratio of $CO_2/H_2/H_2O$ = 1:0.5:0.5 at Pd loading weight of 3.90 wt% under the condition of Xe lamp illumination with UV light. This maximum value is obtained after illumination time of Xe lamp of 6 h. The previous studies reported that the molar quantities of CO per unit weight of photocatalyst in the case of CO_2/H_2O with Pd/TiO_2 were 0.12 μmol/g and 0.13 μmol/g [22,39], while the study reported that the molar quantity of CO per unit weight of photocatalyst in the case of CO_2/H_2 with Pd/TiO_2 was 45 μmol/g [23]. These molar quantities of CO per unit weight of photocatalyst were obtained after illumination of 6 [22], 5 [39], and 3 [23] h, respectively.

Compared to the other studies, CO_2 reduction performance in terms of producing CH_4 or CO per unit weight of photocatalyst obtained in this study does not necessarily imply that the photocatalyst was prepared. Additionally, the best time to obtain the highest molar quantity of produced fuel per unit weight of photocatalsyt is almost the same as the previous studies. However, in terms of producing the other fuels such as C_2H_4 and C_2H_6, which are difficult to produce through CO_2 reduction and were not reported in the other studies, are confirmed in this study. According to the previous study [21], Pd/TiO_2 could produce hydrocarbon such as C_2H_6 more effectively compared to the other photocatalysts. The CO_2 molecules activated at Pd sites react with H^+ and the electrons to produce the intermediate Pd-C=O. Meanwhile, a small amount of CO is generated by C=O desorption, but Pd-C=O further interacts with the dissociated H to form a Pd-C species. Finally, the carbon species generated continue to react with the H species at Pd sites to produce CH_4. During the CH_4 formation process, some intermediates (such as $\cdot CH$, $\cdot CH_2$, and $\cdot CH_3$) are produced, and C_2H_6 is obtained when two $\cdot CH_3$ species interact with each other. Since C_2H_4 and C_2H_6 have high heating values, producing these fuels have a profound significance in CO_2 utilization. Therefore, it can be said that this study has realized the photocatalyst having high CO_2 reduction performance.

Though it is thought that the doped Pd can provide the free electron not only to prevent the recombination of electron and hole produced but also to improve light absorption effect, it is necessary to improve the CO_2 reduction performance further. This study suggests that different metals should be doped on TiO_2 to promote the CO_2 reduction further. The co-doped TiO_2 such as $PbS\text{-}Cu/TiO_2$, $Cu\text{-}Fe/TiO_2$, $Cu\text{-}Ce/TiO_2$, $Cu\text{-}Mn/TiO_2$, and $Cu\text{-}CdS/TiO_2$ were reported to promote the CO_2 reduction performance of TiO_2 with H_2O [4,48]. Then, the promotion of CO_2 reduction performance by different metal doping is expected when the combination of $CO_2/H_2/H_2O$ is considered. For example, Fe which can absorb the shorter wavelength light than Pd can [48] should be co-used since the amount of light absorbed by the photocatalyst can be increased and an effective utilization of wide range light can be realized by the combination of Fe and Pd.

3. Materials and Method

3.1. Preparation of Pd/TiO_2 Photocatalyst

The TiO_2 film used in this study was prepared using the sol-gel and dip-coating procedure [24,49,50]. At first, $[(CH_3)_2CHO]_4Ti$ (95 wt% purification, produced by Nacalai Tesque Co., Kyoto, Japan) of 0.3 mol, anhydrous C_2H_5OH (99.5 wt% purification, produced by Nacalai Tesque Co.) of 2.4 mol, distilled water of 0.3 mol, and HCl (35 wt% purification, produced by Nacalai Tesque Co.) of 0.07 mol were mixed to make the TiO_2 sol solution. As the basis to coat TiO_2 film, the sheet of netlike glass fiber was cut into a disc shape whose diameter and thickness were 50 mm and 1 mm, respectively. The disc shaped netlike glass fiber was then immersed into the TiO_2 sol solution at a speed of 1.5 mm/s and lifted at 0.22 mm/s. The disc was dried and heated at the controlling firing temperature (*FT*) and the firing duration time (*FD*) of 623 K and 180 s, respectively. After the TiO_2 film was coated on netlike glass disc, the pulse arc plasma method was selected to load Pd on the TiO_2 film. The pulse arc plasma gun device (ARL-300, produced by ULVAC, Inc., Suzuka, Japan) with Pd electrode having a diameter of 10 mm was used in this study. The quantity of loaded Pd was controlled by pulse number. In this study, the pulse number was varied from 100 to 500, and Pd loading weight with TiO_2 was measured by EPMA, for each pulse number. It is confirmed that the Pd/TiO_2 film prepared in this way could not be removed from the netlike glass fiber by rubbing. Figure 12 shows the photos of netlike glass disc before and after coating of Pd/TiO_2. Since the sheet of netlike glass disc does not have a scouring structure inside it, the TiO_2 film is coated on the surface of netlike glass fiber and Pd can be deposited on TiO_2 film by pulse arc plasma method.

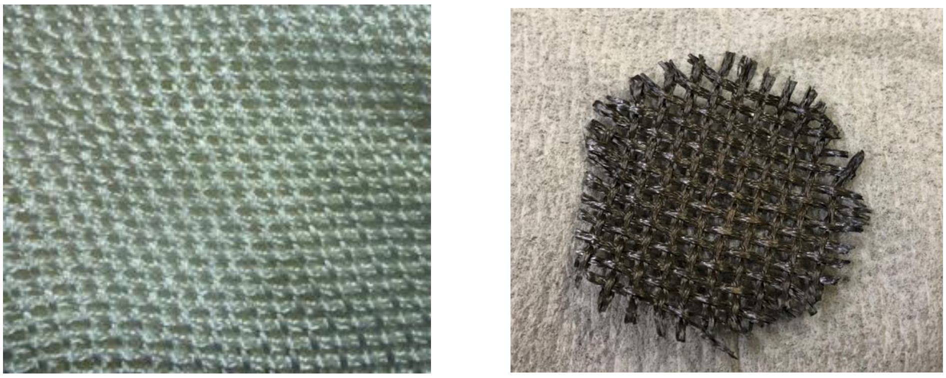

Figure 12. Photos of netlike glass disc before and after coating of Pd/TiO_2 (left: Before; right: After).

3.2. Characterization of Pd/TiO_2 Film

The structural and crystal characteristics of Pd/TiO_2 film prepared were evaluated by using SEM (JXA-8530F, produced by JEOL Ltd., Tokyo, Japan), EPMA (JXA-8530F, produced by JEOL Ltd., Tokyo, Japan), and EELS (JEM-ARM2007 Cold, produced by JEOL Ltd., Tokyo, Japan). In order to analyze the sample by these equipments, carbon was coated on Pd/TiO_2 whose thickness was approximately 15 nm by the dedicated device (JEC-1600, produced by JEOL Ltd.) before analysis. This carbon coating was conducted for analysis, while the CO_2 reduction experiment was carried out without carbon coating. The carbon coating was not conducted for the right photo in Figure 1.

The electron was emitted on the sample by the electron probe applying the acceleration voltage of 15 kV and the current at 3.0×10^{-8} A to analyze the surface structure of the sample by SEM. Simultaneously, EPMA detects the characteristic X-ray. The space resolutions for SEM and EPMA were set at 10 μm. The state of prepared photocatalyst, as well as the quantity of doped metal within TiO_2 film could be known by EPMA analysis.

The electron probe emits electrons to the sample at the acceleration voltage of 200 kV, when the inner structure of the sample is analyzed by STEM. The size, thickness, and structure of loaded Pd were evaluated. The X-ray characteristics of the sample is detected by EDS at the same time. Therefore, the concentration distribution of chemical elements toward thickness direction of the sample is known. In the present paper, the concentration distribution of Ti, Pd, and Si were analyzed.

EELS is used to detect elements, as well as to determine oxidation states of transition metals. The EELS characterization was determined by JEM-ARM200F equipped with GIF Quantum having 2048 ch. The dispersion of 0.5 eV/ch for the full width at half maximum of the zero loss peak was achieved in the study.

3.3. CO_2 Reduction Experiment

Figure 13 shows the experimental setup of the reactor composed of a stainless tube (height of 100 mm and inside diameter of 50 mm), Pd/TiO_2 film coated on netlike glass disc (diameter of 50 mm and thickness of 1 mm) located on the teflon cylinder (height of 50 mm and diameter of 50 mm), a quartz glass disc (diameter of 84 mm and thickness of 10 mm), an edge cut filter cutting off the light whose wavelength is below 400 nm (SCF-49.5C-42L, produced by SIGMA KOKI CO. LTD., Tokyo, Japan), a 150 W Xe lamp (L2175, produced by Hamamatsu Photonics K. K.), mass flow controller, gas cylinder of CO_2 and H_2.

The reactor volume available for CO_2 is 1.25×10^{-4} m^3. The light of Xe lamp which is located outside the stainless tube illuminates Pd/TiO_2 film coated on the netlike glass disc through the edge cut filter and the quartz glass disc that are at the top of the stainless tube. The wavelength of light illuminating by Xe lamp is distributed from 185 nm to 2000 nm. Since an edge cut filter can remove UV components of the light from the Xe lamp, the wavelength from Xe lamp is distributed from 401 to 2000 nm with the filter. Figure 14 shows the spectra data on light intensity of Xe lamp without the edge filter according to the catalog of Xe lamp company. Figure 15 shows the performance of the edge cut filter to cut off the wavelength of light whose wavelength is below 400 nm. The average light intensities of Xe lamp without and with the edge cut filter are 65.0 W/cm^2 and 40.5 W/cm^2, respectively.

CO_2 gas and H_2 gas whose purity were 99.995 vol% and 99.99999 vol%, respectively were controlled by mass flow controller and mixed in the buffer chamber before the experiment. The mixing ratio of CO_2 and H_2 was checked and confirmed by TCD gas chromatograph (Micro GC CP4900, produced by GL Science, Tokyo, Japan) before being introduced into the reactor. The distilled water was then injected into the reactor via gas sampling tap and when Xe lamp was turned on. The water was injected and vaporized by the heat of Xe lamp completely. The molar ratio of CO_2/H_2/H_2O was set at 1:0.5:0.5, 1:0.5:1, 1:1:0.5, 1:1:1, 1:2:2. The temperature in reactor rose up to 343 K within 1 h and was kept at about 343 K during the entire experiment.

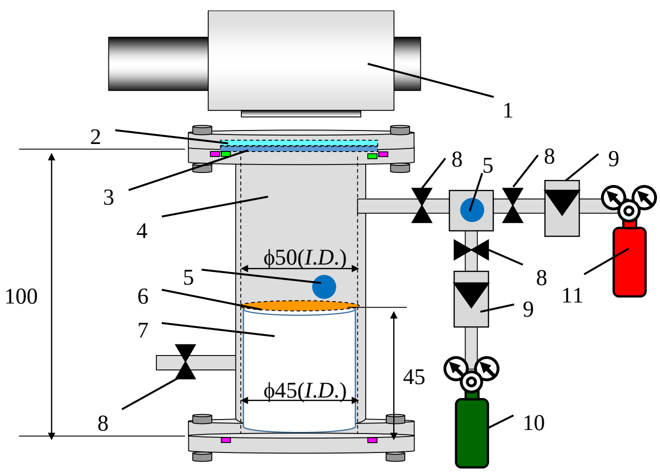

1. Xe lamp, 2. Sharp cut filter, 3. Quartz glass disc, 4. Stainless pipe,
5. Gas sampling tap, 6. Photocatalyst, 7. Teflon cylinder, 8. Valve,
9. Mass flow controller, 10. CO_2 gas cylinder (99.995 vol%),
11. H_2 gas cylinder (99.99999 vol%)

Figure 13. Experimental setup for CO_2 reduction [49,50].

In the CO_2 reduction experiment with UV light, samples of the gas in the reactor were taken every 6 h, while in the CO_2 reduction experiment without UV light samples were taken every 24 h due to the difference of reaction speed of prepared photocatalyst under these two conditions. The gas samples were analyzed using FID gas chromatograph (GC353B, produced by GL Science) and methanizer (MT221, produced by GL Science). FID gas chromatograph and metanizer can be analyzed in the minimum range of 1 ppmV.

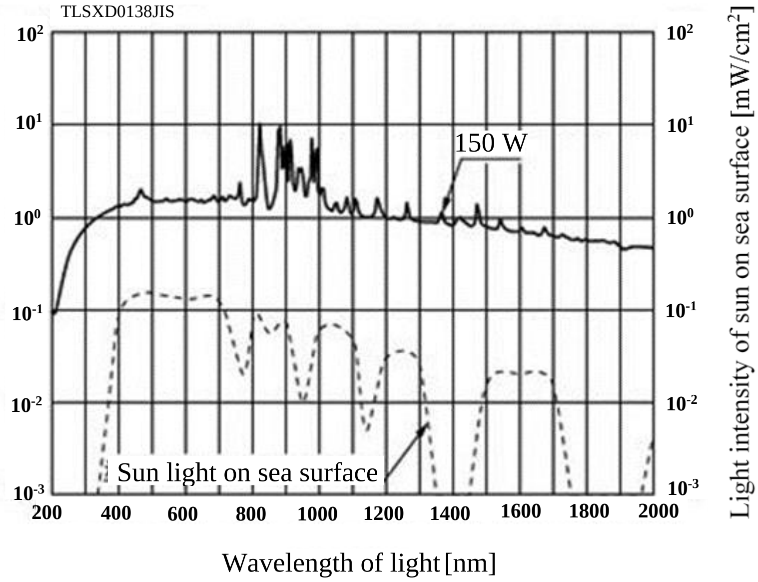

Figure 14. Spectra data on light intensity of Xe lamp without edge filter.

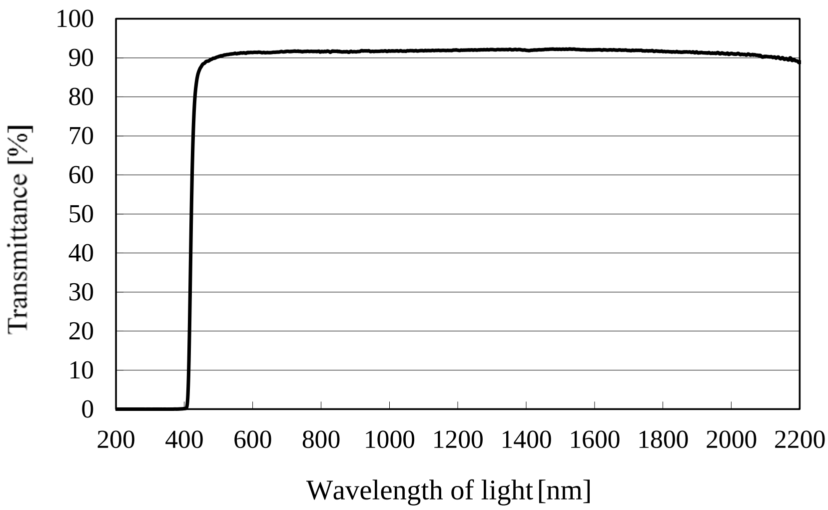

Figure 15. Characterization of edge cut filter to cut off the wavelength of light under 400 nm [49,50].

4. Conclusions

The following conclusions could be drawn from this study:

- The nanosized Pd particles could be loaded on TiO_2 uniformly by the pulse arc plasma method. Pd in Pd/TiO_2 prepared by this method exists in the form of Pd metal.
- The highest CO_2 reduction performance to produce CO, CH_4, C_2H_4, and C_2H_6 was obtained at the molar ratio of CO_2/H_2/H_2O = 1:0.5:0.5 with Xe lamp illumination with or without UV light. It is revealed that the molar ratio of CO_2/total reductants = 1:1 is the optimum to produce fuels.
- The maximum molar quantity of fuel per unit weight of photocatalyst is obtained at Pd loading weight of 3.90 wt% irrespective of fuel type. In this study, the maximum molar quantities of CO and CH_4 per unit weight of photocatalyst were 30.3 µmol/g and 22.1 µmol/g, respectively, for the molar ratio of CO_2/H_2/H_2O = 1:0.5:0.5 at Pd loading weight of 3.90 wt% under the condition of Xe lamp illumination with UV light.

- The Pd/TiO_2 photocatalyst prepared in this study could produce C_2H_4 and C_2H_6, as well as CO and CH_4, therefore, it can be said that the photocatalyst prepared in this study has realized to have the higher CO_2 reduction performance.

Author Contributions: Data curation, T.I. and Y.S.; methodology, A.K.; supervision, M.H.; writing—original draft, A.N.; writing—review and editing, E.H. All authors have read and agreed to the published version of the manuscript.

Funding: This research received no external funding.

Conflicts of Interest: The author declares no conflict of interest.

References

1. Greenhouse Gases Observing Satellite GOAST "IBUSUKI1:0.5:0.5". Available online: http://www.goast.nies.go.jp/en/ (accessed on 5 February 2020).
2. Tahir, M.; Amin, N.S. Indium-doped TiO_2 nanoparticles for photocatalytic CO_2 reduction with H_2O vapors to CH_4. *Appl. Catal. B Environ.* **2015**, *162*, 98–109. [CrossRef]
3. Abdullah, H.; Khan, M.R.; Ong, H.R.; Yaakob, Z. Modified TiO_2 photocatalyst for CO_2 photocatalytic reduction: An overview. *J. CO_2 Util.* **2017**, *22*, 15–32. [CrossRef]
4. Sohn, Y.; Huang, W.; Taghipour, F. Recent progress and perspectives in the photocatalytic CO_2 reduction of Ti-oxide-based nanomaterials. *Appl. Surf. Sci.* **2017**, *396*, 1696–1711. [CrossRef]
5. Nahar, S.; Zain, M.F.M.; Kadhum, A.A.H.; Abu Hasan, H. Advances in Photocatalytic CO_2 Reduction with Water: A Review. *Materials* **2017**, *10*, 629. [CrossRef]
6. Ola, O.; Maroto-Valer, M. Review of material design and reactor engineering on TiO_2 photocatalysis for CO_2 reduction. *J. Photochem. Photobiol. C Photochem. Rev.* **2015**, *24*, 16–42. [CrossRef]
7. Xie, S.; Wang, Y.; Zhang, Q.; Deng, W.; Wang, Y. MgO- and Pt-Promoted TiO_2 as an Efficient Photocatalyst for the Preferential Reduction of Carbon Dioxide in the Presence of Water. *ACS Catal.* **2014**, *4*, 3644–3653. [CrossRef]
8. Khalid, N.; Ahmed, E.; Niaz, N.; Nabi, G.; Ahmad, M.; Tahir, M.B.; Rafique, M.; Rizwan, M.; Khan, Y. Highly visible light responsive metal loaded N/TiO_2 nanoparticles for photocatalytic conversion of CO_2 into methane. *Ceram. Int.* **2017**, *43*, 6771–6777. [CrossRef]
9. Tan, L.-L.; Ong, W.-J.; Chai, S.-P.; Mohamed, A.R. Noble metal modified reduced graphene oxide/TiO_2 ternary nanostructures for efficient visible-light-driven photoreduction of carbon dioxide into methane. *Appl. Catal. B Environ.* **2015**, *166*, 251–259. [CrossRef]
10. Camarillo, R.; Tostón, S.; Martínez, F.; Jiménez, C.; Rincón, J. Improving the photo-reduction of CO_2 to fuels with catalysts synthesized under high pressure: Cu/TiO_2. *J. Chem. Technol. Biotechnol.* **2017**, *93*, 1237–1248. [CrossRef]
11. Aguirre, M.E.; Zhou, R.; Eugene, A.J.; Guzman, M.I.; Grela, M.A. Cu_2O/TiO_2 heterostructures for CO_2 reduction through a direct Z-scheme: Protecting Cu_2O from photocorrosion. *Appl. Catal. B Environ.* **2017**, *217*, 485–493. [CrossRef]
12. Marcì, G.; García-López, E.I.; Palmisano, L. Photocatalytic CO_2 reduction in gas–solid regime in the presence of H_2O by using GaP/TiO_2 composite as photocatalyst under simulated solar light. *Catal. Commun.* **2014**, *53*, 38–41. [CrossRef]
13. Beigi, A.A.; Fatemi, S.; Salehi, Z. Synthesis of nanocomposite CdS/TiO_2 and investigation of its photocatalytic activity for CO_2 reduction to CO and CH_4 under visible light irradiation. *J. CO_2 Util.* **2014**, *7*, 23–29. [CrossRef]
14. Fang, Z.; Li, S.; Gong, Y.; Liao, W.; Tian, S.; Shan, C.; He, C. Comparison of catalytic activity of carbon-based AgBr nanocomposites for conversion of CO_2 under visible light. *J. Saudi Chem. Soc.* **2014**, *18*, 299–307. [CrossRef]
15. Xu, F.; Zhang, J.; Zhu, B.; Yu, J.; Xu, J. $CuInS_2$ sensitized TiO_2 hybrid nanofibers for improved photocatalytic CO_2 reduction. *Appl. Catal. B Environ.* **2018**, *230*, 194–202. [CrossRef]
16. Camarillo, R.; Tostón, S.; Martínez, F.; Jiménez, C.; Rincón, J. Preparation of TiO_2-based catalysts with supercritical fluid technology: Characterization and photocatalytic activity in CO_2 reduction. *J. Chem. Technol. Biotechnol.* **2017**, *92*, 1710–1720. [CrossRef]

17. Tostón, S.; Camarillo, R.; Martínez, F.; Jiménez, C.; Rincón, J. Supercritical synthesis of platinum-modified titanium dioxide for solar fuel production from carbon dioxide. *Chin. J. Catal.* **2017**, *38*, 636–650. [CrossRef]
18. Jiao, J.; Wei, Y.; Zhao, Y.; Zhao, Z.; Duan, A.; Liu, J.; Pang, Y.; Li, J.; Jiang, G.; Wang, Y. AuPd/3DOM-TiO_2 catalysts for photocatalytic reduction of CO_2: High efficient separation of photogenerated charge carriers. *Appl. Catal. B Environ.* **2017**, *209*, 228–239. [CrossRef]
19. Camarillo, R.; Tostón, S.; Martínez, F.; Jiménez, C.; Rincón, J. Enhancing the photocatalytic reduction of CO_2 through engineering of catalysts with high pressure technology: Pd/TiO_2 photocatalysts. *J. Supercrit. Fluids* **2017**, *123*, 18–27. [CrossRef]
20. Chen, W.; Wang, Y.; Shangguan, W. Metal (oxide) modified (M = Pd, Ag, Au and Cu) $H_2SrTa_2O_7$ for photocatalytic CO_2 reduction with H_2O: The effect of cocatalysts on promoting activity toward CO and H_2 evolution. *Int. J. Hydrog. Energy* **2019**, *44*, 4123–4132. [CrossRef]
21. Yu, Y.; Lan, Z.; Guo, L.; Wang, E.; Yao, J.; Cao, Y. Synergistic effects of Zn and Pd species in TiO_2 towards efficient photo-reduction of CO_2 into CH_4. *New J. Chem.* **2018**, *42*, 483–488. [CrossRef]
22. Singhal, N.; Kumar, U. Noble metal modified TiO_2: Selective photoreduction of CO_2 to hydrocarbons. *Mol. Catal.* **2017**, *439*, 91–99. [CrossRef]
23. Li, N.; Liu, M.; Yang, B.; Shu, W.; Shen, Q.; Liu, M.; Zhou, J. Enhanced photocatalytic performance toward CO_2 hydrogeneration over nanosized TiO_2-loaded Pd under UV irradiation. *J. Phys. Chem.* **2017**, *121*, 2923–2932.
24. Nishimura, A.; Inoue, T.; Sakakibara, Y.; Hirota, M.; Koshio, A.; Kokai, F.; Hu, E. Optimum molar ratio of H_2 and H_2O to reduce CO_2 using Pd/TiO_2. *AIMS Mater. Sci.* **2019**, *6*, 464–483. [CrossRef]
25. Tasbihi, M.; Schwarze, M.; Edelmannová, M.; Spoeri, C.; Strasser, P.; Schomäcker, R. Photocatalytic reduction of CO_2 to hydrocarbons by using photodeposited Pt nanoparticles on carbon-doped titania. *Catal. Today* **2019**, *328*, 8–14. [CrossRef]
26. Su, K.-Y.; Chen, C.-Y.; Wu, R.-J. Preparation of Pd/TiO2 nanowires for the photoreduction of CO_2 into renewable hydrocarbon fuels. *J. Taiwan Inst. Chem. Eng.* **2019**, *96*, 409–418. [CrossRef]
27. Goren, Z.; Willner, I.; Nelson, A.J.; Frank, A.J. Selective photoreduction of CO_2/HCO_3^- to Formate by Aqueous Suspensions and Colloids of Pd-TiO_2. *J. Phys. Chem.* **1990**, *94*, 3784–3790. [CrossRef]
28. Tseng, I.-H.; Chang, W.-C.; Wu, J.C.S. Photoreduction of CO_2 using sol–gel derived titania and titania-supported copper catalysts. *Appl. Catal. B Environ.* **2002**, *37*, 37–48. [CrossRef]
29. Nishimura, A.; Sugiura, N.; Fujita, M.; Kato, S.; Kato, S. Influence of Preparation Conditions of Coated TiO_2 Film on CO_2 Reforming Performance. *Kagaku Kogaku Ronbunshu* **2007**, *33*, 146–153. [CrossRef]
30. Izumi, Y. Recent advances in the photocatalytic conversion of carbon dioxide to fuels with water and/or hydrogen using solar energy and beyond. *Co-ord. Chem. Rev.* **2013**, *257*, 171–186. [CrossRef]
31. Lo, C.-C.; Hung, C.-H.; Yuan, C.-S.; Wu, J.-F. Photoreduction of carbon dioxide with H_2 and H_2O over TiO_2 and ZrO_2 in a circulated photocatalytic reactor. *Sol. Energy Mater. Sol. Cells* **2007**, *91*, 1765–1774. [CrossRef]
32. Mahmodi, G.; Sharifnia, S.; Madani, M.; Vatanpour, V. Photoreduction of carbon dioxide in the presence of H_2, H_2O and CH_4 over TiO_2 and ZnO photocatalysts. *Sol. Energy* **2013**, *97*, 186–194. [CrossRef]
33. Jensen, J.; Mikkelsen, M.; Krebs, F.C. Flexible substrates as basis for photocatalytic reduction of carbon dioxide. *Sol. Energy Mater. Sol. Cells* **2011**, *95*, 2949–2958. [CrossRef]
34. Wu, H.Y.; Bai, H.; Wu, J.C.S. Photocatalytic reduction of CO_2 using Ti-MCM-41 Photocatalysis in Monoethanolamine Solution for Methane Production. *Ind. Eng. Chem. Res.* **2014**, *53*, 11221–11227. [CrossRef]
35. Korzhak, A.V.; Ermokhina, N.I.; Stroyuk, A.L.; Bukhtiyarov, V.K.; Raevskaya, A.E.; Litvin, V.I.; Kuchmiy, S.Y.; Ilyin, V.G.; Manorik, P.A. Photocatalytic hydrogen evolution over mesoporous TiO_2/metal nanocomposites. *J. Photochem. Photobiol. A Chem.* **2008**, *198*, 126–134. [CrossRef]
36. Nishimura, A.; Tatematsu, D.; Toyoda, R.; Hirota, M.; Koshio, A.; Kokai, F.; Hu, E. Effect of overlapping layout of Fe/TiO_2 on CO_2 reduction with H_2 and H_2O. *Mof Sol. Photoen.* **2019**, *3*, 1–8.
37. Feng, H.; Xu, H.; Feng, H.; Gao, Y.; Jin, X. The sol-gel synthesis and photocatalytic activity of Gd-SiO_2-TiO_2 photocatalyst. *Chem. Phys. Lett.* **2019**, *733*, 136676. [CrossRef]
38. Wang, D.; Zhou, W.; McCaughy, B.; Hampsey, J.; Ji, X.; Jiang, Y.-B.; Xu, H.; Tang, J.; Schmehl, R.; O'Connor, C.; et al. Electrodeposition of Metallic Nanowire Thin Films Using Mesoporous Silica Templates. *Adv. Mater.* **2003**, *15*, 130–133. [CrossRef]

39. Yui, T.; Kan, A.; Saitoh, C.; Koike, K.; Ibusuki, T.; Ishitani, O. Photochemical Reduction of CO_2 Using TiO_2: Effects of Organic Adsorbates on TiO_2 and Deposition of Pd onto TiO_2. *ACS Appl. Mater. Interfaces* **2011**, *3*, 2594–2600. [CrossRef]
40. Kočí, K.; Matějová, L.; Reli, M.; Čapek, L.; Matějka, V.; Lacný, Z.; Kuśtrowski, P.; Obalová, L. Sol–gel derived Pd supported TiO_2-ZrO_2 and TiO_2 photocatalysts; their examination in photocatalytic reduction of carbon dioxide. *Catal. Today* **2014**, *230*, 20–26. [CrossRef]
41. Nishimura, A.; Ishida, N.; Tatematsu, D.; Hirota, M.; Koshio, A.; Kokai, F.; Hu, E. Effect of Fe Loading Condition and Reductants on CO_2 Reduction Performance with Fe/TiO_2 Photocatalyst. *Int. J. Photoenergy* **2017**, *2017*, 1–11. [CrossRef]
42. Zhao, H.; Rao, G.; Wang, L.; Xu, J.; Liu, L.; Li, Y. Synthesis of novel MgAl layered double oxide grafted TiO_2 cuboids and their photocatalytic activity on CO_2 reduction with water vapor. *Catal. Sci. Technol.* **2015**, *5*, 3288–3295. [CrossRef]
43. Zhang, R.; Huang, Z.; Li, C.; Zuo, Y.; Zhou, Y. Monolithic g-C_3N_4/reduced graphene oxide aerogel with in situ embedding of Pd nanoparticles for hydrogenation of CO_2 to CH_4. *Appl. Surf. Sci.* **2019**, *475*, 953–960. [CrossRef]
44. Kulandaivalu, T.; Rashid, S.A.; Sabli, N.; Tan, T.L. Visible light assisted photocatalytic reduction of CO_2 to ethane using CQDS/Cu_2O nanocomosite photocatalyst. *Diam. Relat. Mater.* **2019**, *91*, 64–73. [CrossRef]
45. Zhu, Z.; Huang, W.-R.; Chen, C.-Y.; Wu, R.-J. Preparation of Pd–Au/TiO_2–WO_3 to enhance photoreduction of CO_2 to CH_4 and CO. *J. CO_2 Util.* **2018**, *28*, 247–254. [CrossRef]
46. Tasbihi, M.; Fresno, F.; Simon, U.; Villar-Garcia, I.J.; Pérez-Dieste, V.; Escudero, C.; O'Shea, V.A.D.L.P. On the selectivity of CO_2 photoreduction towards CH_4 using Pt/TiO_2 catalysts supported on mesoporous silica. *Appl. Catal. B Environ.* **2018**, *239*, 68–76. [CrossRef]
47. Wei, Y.; Wu, X.; Zhao, Y.; Wang, L.; Zhao, Z.; Huang, X.; Liu, J.; Li, J. Efficient photocatalyst of TiO_2 nanocrystals-supported PtRu alloy nanoparticles for CO_2 reduction with H_2O: Synergetic effect of Pt-Ru. *Appl. Catal. B Environ.* **2018**, *236*, 445–457. [CrossRef]
48. Tahir, M.; Amin, N.S. Advances in visible light responsive titanium oxide-based photocatalysts for CO_2 conversion to hydrocarbon fuels. *Energy Convers. Manag.* **2013**, *76*, 194–214. [CrossRef]
49. Nishimura, A.; Toyoda, R.; Tatematsu, D.; Hirota, M.; Koshio, A.; Kokai, F.; Hu, E. Effect of molar ratio of H_2 and H_2O on CO_2 reduction characteristics of overlapped Cu/TiO_2. *Int. J. Eng. Sci. Invent.* **2018**, *7*, 18–28.
50. Japan Society of Mechanical Engineering. *JSME Heat Transfer Handbook*, 1st ed.; Maruzen: Tokyo, Japan, 1993; pp. 366–369.

Sample Availability: Samples of the compounds are not available from the authors.